nature sustainability

ARTICLES

https://doi.org/10.1038/s41893-020-0562-1

Check for updates

Dust pollution from the Sahara and African infant mortality

Sam Heft-Neal[1], Jennifer Burney[2], Eran Bendavid[3], Kara K. Voss[4] and Marshall Burke[1,5,6] ✉

Estimation of pollution impacts on health is critical for guiding policy to improve health outcomes. Estimation is challenging, however, because economic activity can worsen pollution but also independently improve health outcomes, confounding pollution–health estimates. We leverage variation in exposure to local particulate matter of diameter <2.5 μm ($PM_{2.5}$) across Sub-Saharan Africa driven by distant dust export from the Sahara, a source uncorrelated with local economic activity. Combining data on a million births with local-level estimates of aerosol particulate matter, we find that an increase of 10 μg m^{-3} in local annual mean $PM_{2.5}$ concentrations causes a 24% increase in infant mortality across our sample (95% confidence interval: 10–35%), similar to estimates from wealthier countries. We show that future climate change driven changes in Saharan rainfall—a control on dust export—could generate large child health impacts, and that seemingly exotic proposals to pump and apply groundwater to Saharan locations to reduce dust emission could be cost competitive with leading child health interventions.

Poor air quality is a known determinant of poor health outcomes, with even modest improvements in air quality likely to save millions of premature deaths annually[1,2]. Children younger than 5 yr are particularly vulnerable and impacts are thought to be largest in developing regions where exposure to high levels of ambient air pollution during childhood is estimated to reduce overall life expectancy by 4–5 yr on average[3]. However, while quantitative assessment of the harms from pollution exposure has greatly improved in recent years, only recently have researchers begun using quasi-experimental research designs that plausibly isolate variation in ambient pollution exposure from other correlated factors that also affect health[4–9]. Most of these estimates are concentrated in wealthy regions or limited to relatively wealthy cities in developing countries where data are available.

Direct estimation of the local health burdens of air pollution exposures requires addressing two challenges. The first challenge is accurately measuring both exposures and responses, which has become easier with both advances in remote sensing of air quality[10] and the accumulation of georeferenced household survey-based health measurements across broad geographies[11]. The second challenge is disentangling pollution exposures from other correlated variables that might also directly affect health. In particular, many economic activities (for example, transportation, industrial production and biomass clearing in agriculture) produce particulate matter of diameter <2.5 μm ($PM_{2.5}$) locally but can also directly affect health outcomes by changing the economic status of households. These direct effects could positively affect child health, for instance if higher incomes enable greater access or use of health services, or negatively affect child health if, for example, economically engaged adults are less able to invest time in childrens' well-being[12].

To disentangle the impact of covarying factors on infant mortality, researchers have used study designs that leverage setting-specific sources of variation in $PM_{2.5}$ that are likely uncorrelated with other factors that affect health outcomes[4–9]. These approaches use, for example, changes in environmental policy[6,9], naturally occurring local weather phenomena[5] and traffic patterns[7] as sources of plausibly exogenous variation in air quality. However, given that these approaches rely on often idiosyncratic local-level events for variation, they are difficult to apply across larger spatiotemporal scales. To build a broader understanding, recent quasi-experimental studies have used local variation in $PM_{2.5}$ derived from natural sources such as dust and argued that this approach allows for causal interpretation of $PM_{2.5}$ impacts on health across broad developing-country geographies[13,14]. While using local-level variation in $PM_{2.5}$ from natural sources helps mitigate some concerns of economic activity as a confound, these studies—with the exception of a related paper[15] that uses reanalysis data to estimate Saharan dust transport to population centres—have no explicit way of distinguishing locally sourced $PM_{2.5}$ from distant $PM_{2.5}$ using direct measurement (see Supplementary Information for additional discussion of the related literature). As a result, the possibility remains that existing estimates in these developing-country settings[2,13], which are critical for understanding global health burdens and evaluating policy choices, could be biased by unobserved local economic activity. Existing works also provide little guidance on how impacts from naturally sourced $PM_{2.5}$ might be mitigated.

Here we combine household survey-based data on the location and timing of nearly one million births across Africa with changes in local $PM_{2.5}$ levels driven by remote dust activation events in the Bodélé Depression in Chad. The Bodélé Depression is the single largest source of dust emissions in the world, including substantial intercontinental transmission[16,17], and is thousands of kilometres away from most of the observed births in our study (Extended Data Fig. 1). Using dust emission from the Bodélé allows us to isolate the impact of poor air quality from local unobserved covarying factors that might also affect child health. Dust propagation from the Bodélé is associated with variation in climactic and circulation conditions in the Sahara[18–20], including variation in local rainfall and in strong winds funneled between nearby mountain ranges. Activation events propagate dust from the Bodélé across much of West Africa over a matter of days (Extended Data Fig. 2a)[21] and remotely sensed dust aerosol optical depth (DAOD) data[20] indicate that these activation events are

[1]Center on Food Security and the Environment, Stanford University, Stanford, CA, USA. [2]School of Global Policy and Strategy, UC San Diego, La Jolla, CA, USA. [3]School of Medicine, Stanford University, Stanford, CA, USA. [4]Scripps Institution of Oceanography, UC San Diego, La Jolla, CA, USA. [5]Department of Earth System Science, Stanford University, Stanford, CA, USA. [6]National Bureau of Economic Research, Cambridge, MA, USA. ✉e-mail: mburke@stanford.edu

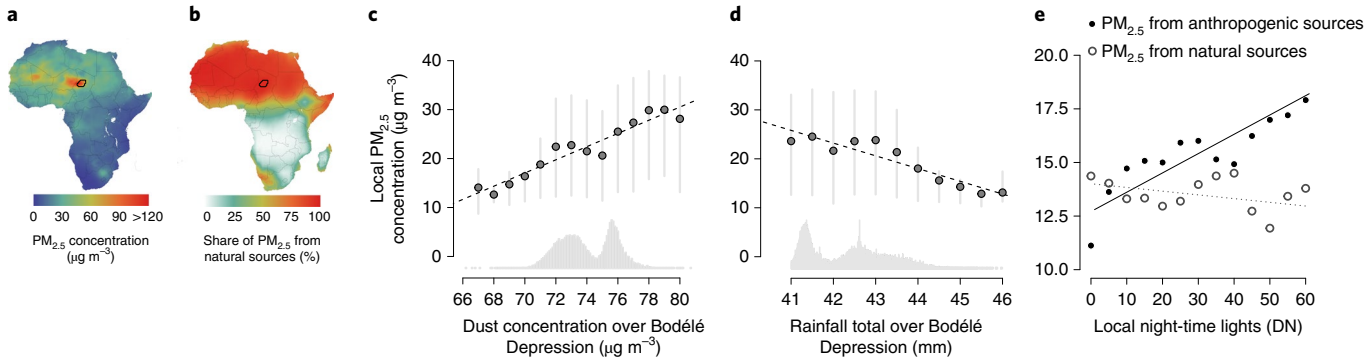

Fig. 1 | Local air pollution in Africa is driven by both local economic activity and remote natural sources. a, Average annual $PM_{2.5}$ concentration during 2001–2015[10], with the Bodélé Depression outlined in black. **b**, The share of $PM_{2.5}$ estimated to come from natural sources[10], with the Bodélé Depression outlined in black. **c**, Higher dust concentrations over the Bodélé are associated with higher local $PM_{2.5}$ concentrations in our study locations. Annual observations of dust concentrations over the Bodélé were divided into equal-sized bins and the average annual $PM_{2.5}$ concentrations (points) and interquartile ranges (grey lines) over all survey locations were calculated within each of these bins. Years with more dust in the Bodélé Depression are associated with higher average $PM_{2.5}$ concentrations across Africa. The histogram plotted in the bottom in grey indicates the distribution of dust concentration exposures in our data. **d**, Analogous to **c** using rainfall totals over the Bodélé in place of dust concentrations, showing that higher Bodélé rainfall totals are associated with lower local $PM_{2.5}$ concentrations in our study locations. The histogram plotted in the bottom indicates the distribution of rainfall totals over the Bodélé in our data. **e**, Binned scatterplot of night-time light intensity measured as unit-less digital number (DN) and $PM_{2.5}$ concentrations by source in our study locations. Night-time light intensity was assigned to one-unit bins and average $PM_{2.5}$ concentrations were calculated within each bin separately for anthropogenic and naturally sourced (dust and sea salt) $PM_{2.5}$. Higher night-time light intensity is associated with higher local concentrations of $PM_{2.5}$ from anthropogenic sources (solid line) but not with higher $PM_{2.5}$ from natural sources (dotted line).

a substantial driver of local DAOD levels across much of Africa, with dissipating intensity over space and time (Extended Data Fig. 2b).

While dust is transported on a daily timescale, satellite retrievals of aerosols, such as dust, are not available under cloud cover and are available within a limited horizontal distance from the satellite track. These gaps in coverage can be partially mitigated by aggregating over longer time spans. To study the impacts of dust on health, we therefore use recently developed annually aggregated estimates of particulate exposure[22]. These data incorporate retrievals from MODIS AOD as well as other satellite instruments (MISR, SeaWIFS) to estimate annual bias-corrected average surface $PM_{2.5}$ concentrations at $0.01^{\circ} \times 0.01^{\circ}$ spatial resolution across the globe and use models to partition these $PM_{2.5}$ concentrations into natural (dust and sea salt) and non-natural sources[10]. We validate these partitions against independent ground station data, finding strong correlations between estimated and observed average dust shares across station locations in our study countries (see Supplementary Information and Extended Data Fig. 3).

While dust export from the Bodélé Depression is highest during the November–March Harmattan season, the Bodélé is one of the only major African dust sources that is active year-round. Emissions from the Bodélé contribute greatly to annual average $PM_{2.5}$ concentrations across much of Africa, particularly in the north and west where natural sources account for >75% of total $PM_{2.5}$ (Fig. 1a,b). Annual variation in dust concentrations and rainfall over the Bodélé correlate strongly with temporal variation in the $PM_{2.5}$ concentrations across our African study locations (Fig. 1c,d). While exported dust is one of the many factors affecting $PM_{2.5}$ concentrations in our sample, the motivation for using natural $PM_{2.5}$ from the Bodélé as a source of variation is that emissions from distant natural sources are less likely to be correlated with confounding local economic activity than emissions from local anthropogenic (or natural) sources. Indeed, while we find a positive time-series correlation in our study locations between estimates of $PM_{2.5}$ concentrations from anthropogenic sources and night-time lights (a proxy for local economic activity), the same correlation does not exist between night-time lights and $PM_{2.5}$ concentrations derived from remote natural sources (Fig. 1e).

To estimate the impact of local $PM_{2.5}$ exposure on health outcomes, we adopt an instrumental variable approach that uses remote variation in dust concentrations (which we take as a proxy for emission) or rainfall to generate exogenous local variation in $PM_{2.5}$, which we then link to observed health outcomes (Methods). Our estimation strategy first uses the product of time-varying dust $PM_{2.5}$ concentrations over the Bodélé Depression and spatially varying average shares of local $PM_{2.5}$ from natural sources to predict local-level $PM_{2.5}$ exposure over the 12 months following each observed birth in our data. We then study whether these predicted $PM_{2.5}$ levels explain the likelihood a child survives to her first birthday, using georeferenced data from the Demographic and Health Surveys (DHS) on the location and timing of 990,696 births across 30 countries and 15 yr (Extended Data Fig. 1; Methods). These household survey data do not allow us to observe cause of death and our estimates thus represent impacts on all-cause infant mortality; it is likely that exposure to air pollution affects health through multiple pathways[13].

For this two-stage estimation procedure to recover the causal effect of variation in air quality on infant health, it must be the case that variation in dust over the Bodélé is strongly correlated with downstream local air quality and that variation in dust over the Bodélé is uncorrelated with other factors beyond local air quality that might also impact child health in that location. To help ensure that this later requirement is met, both estimation stages control for additional factors that could possibly be correlated with both remote dust concentrations and local air quality. These include time-varying measures of local temperature and rainfall, as well as a large set of fixed effects (dummy variables) that account for any additional time-invariant differences in ambient $PM_{2.5}$ and mortality across locations (for example, due to differences in climate or average economic development), local seasonality in both air quality and mortality, and trending factors or abrupt shocks common to all locations in our sample (for example, overall improvements in health services). Additional robustness tests control for global climate phenomena (for example, El Niño/Southern Oscillation, ENSO) that could possibly be correlated with both Saharan dust emission and local health outcomes (Methods). We emphasize that,

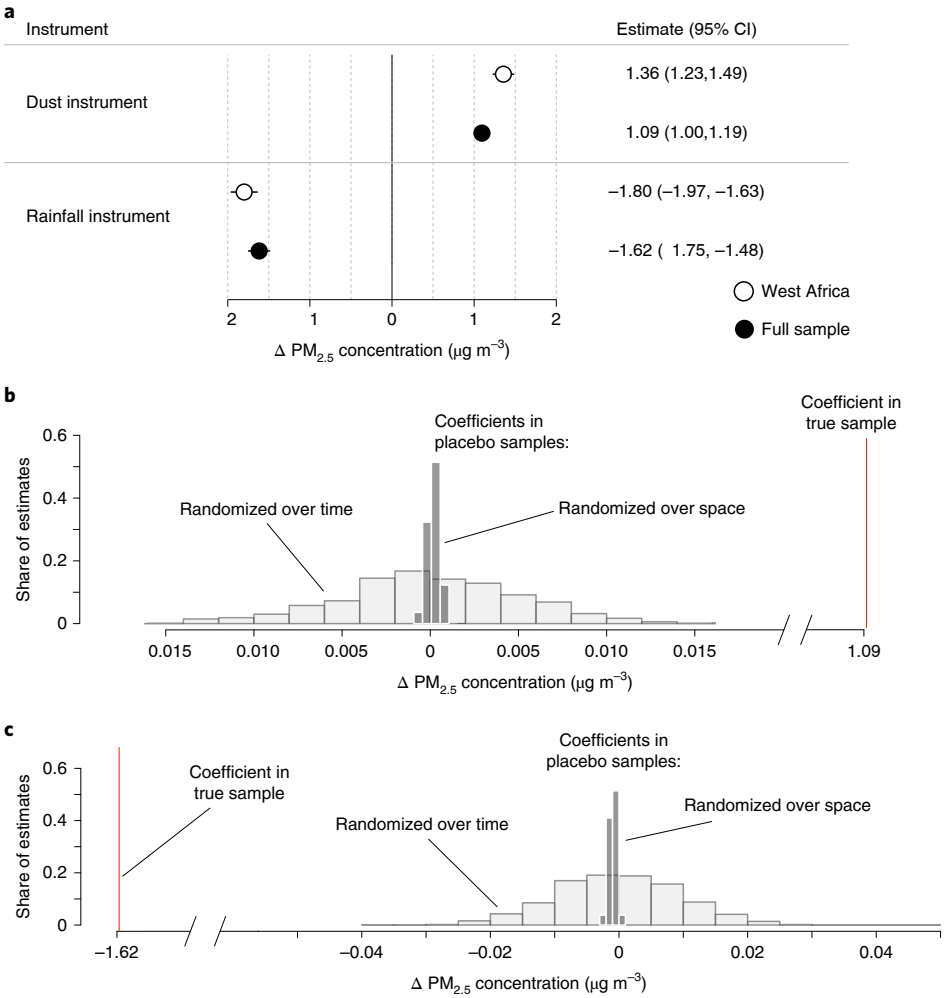

Fig. 2 | Variation in dust and rainfall over the Bodélé Depression are strong predictors of variation in $PM_{2.5}$ concentrations elsewhere in Africa. **a**, First-stage estimates corresponding to λ in equation (1) show the effect of a one-unit change in dust and rainfall instruments on $PM_{2.5}$ concentrations across our study locations. Effects are larger in West Africa, closer to and downwind from the Bodélé Depression. **b**, In a placebo test, we find no effect of Bodélé dust on local $PM_{2.5}$ when we randomly reorder the time series of Bodélé dust (light grey histogram, 1,000 resamples) or when we randomly re-sort shares of $PM_{2.5}$ concentrations across space (dark grey histogram, 1,000 resamples); estimates for both placebo experiments are centred around zero and several orders of magnitude smaller than the effect estimated with the true ordering. **c**, Analogous to **b** but with our rainfall instrument.

to estimate the impact of dust exposure on infant mortality, it is not necessary for us to observe and directly control for all other factors that might contribute to mortality risk. Instead, the key requirement is an ability to isolate dust exposure from other correlated factors that might affect mortality and the purpose of the instrumental variables procedure is to do just that.

Results

Annual variation in dust concentrations in the Bodélé Depression is strongly and positively associated with $PM_{2.5}$ variation in the locations where births are observed in our data, even after conditioning on a broad set of time-invariant and time-varying controls (Fig. 2). We find analogous relationships when we use time-varying measures of rainfall accumulation over the Bodélé Depression rather than direct measures of dust concentration as our source of temporal variation; higher rainfall is known to reduce dust emission in the region[23]. These relationships are robust to the inclusion of rainfall and temperature in the birth locations and to the inclusion of global ENSO variation. Results are similar when we restrict our analysis to exposure comparisons between siblings within the same household by including mother fixed effects (Extended Data Fig. 4). Consistent with the short timescale of dust transmission, we do not find meaningful associations between $PM_{2.5}$ concentrations in our study locations and dust concentrations or rainfall in the Bodélé Depression in the previous year. These robust estimated relationships are consistent with existing understanding of the role the Bodélé Depression plays in propagating dust throughout the region[18,19,21,24].

To further test whether this strong relationship between remote dust emission and local $PM_{2.5}$ concentrations is driven by common time trends, common year-specific shocks across dusty locations or by average spatial differences between dusty and less-dusty locations, we conduct a placebo exercise where we randomly reorder either the time series of dust emissions over the Bodélé or the spatial shares of baseline levels of dust exposure and re-estimate the relationship between these placebo instruments and local-level $PM_{2.5}$ concentrations (Methods). In all cases, estimates on these placebo samples ($n = 1{,}000$ for each type of reshuffling) are close to zero (Fig. 2b,c), suggesting our estimated relationships between local $PM_{2.5}$ concentrations and remote dust emission are not spurious.

We then use this predicted variation in local $PM_{2.5}$ driven by remote dust emission to estimate the impact of $PM_{2.5}$ on local health

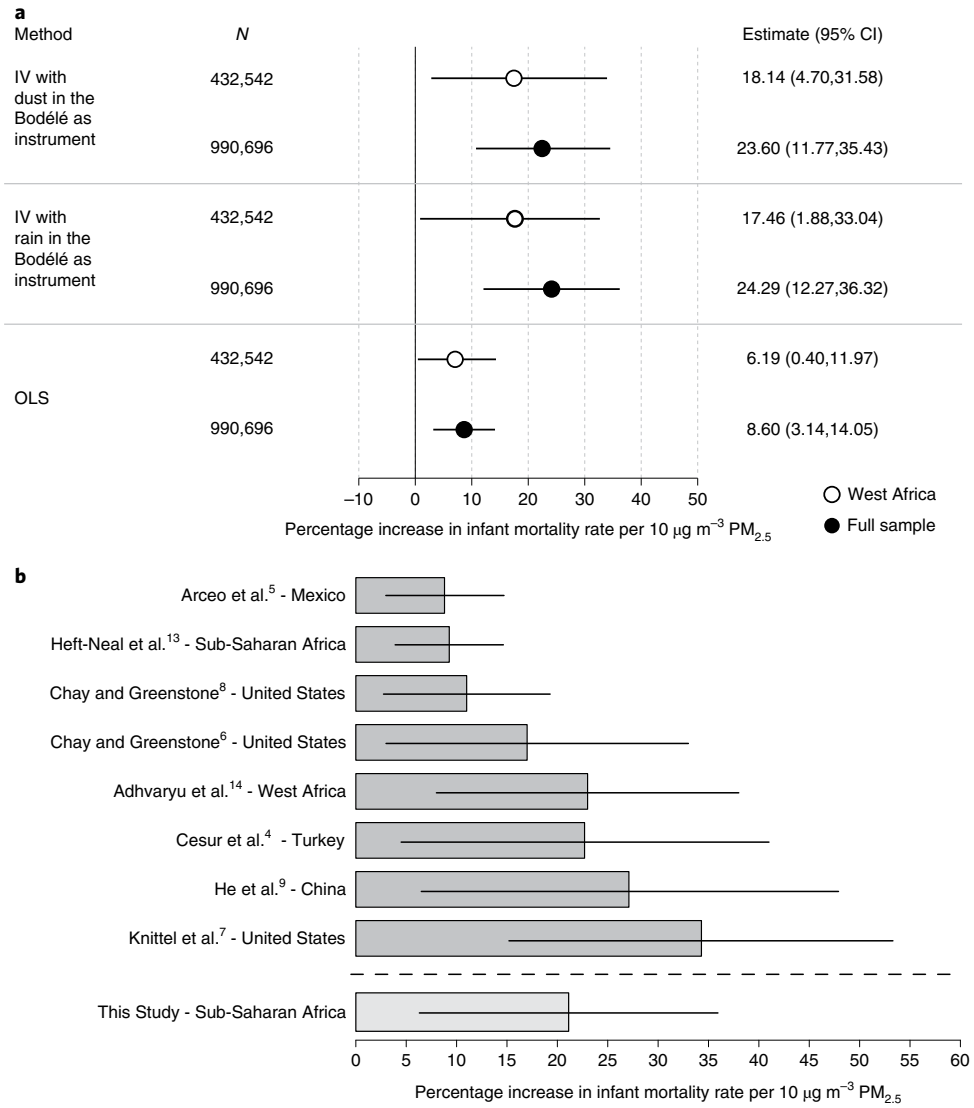

Fig. 3 | Instrumental variables (IV) estimates suggest large impacts of $PM_{2.5}$ on infant mortality, with effect sizes similar to quasi-experimental studies from higher income countries. a, IV estimates corresponding to β in equation (2) indicate a 10 μg m^{-3} increase in $PM_{2.5}$ concentration causes infant mortality to rise by 18% in West Africa and 24% across the full Sub-Saharan Africa sample; IV estimates are substantially larger than OLS estimates and are statistically different at the 95% CI in the full Sub-Saharan Africa sample ($P = 0.02$ for dust instrument and $P = 0.03$ for rainfall instrument). The P values for the difference between β_{IV} and β_{OLS} in the West African sample are 0.06 and 0.17 for dust and rainfall instruments, respectively. Both IV and OLS estimates include DHS cluster, birth year and country–month fixed effects as well as household, mother and child controls (see Methods). **b**, IV estimates are larger and statistically different than previous estimates for all of Sub-Saharan Africa and similar to recent results for West Africa and to causal estimates in other parts of the world with higher incomes.

outcomes. We estimate that an increase of 10 μg m^{-3} in local ambient $PM_{2.5}$ concentration causes a 24% rise in infant mortality across our full sample (95% confidence interval (CI): 10–35%) and a 17% rise in our West Africa sample (95% CI: 2–33%; Fig. 3a). Our results are similar whether we use either dust emission or rainfall over the Bodélé as our instrument, and are again robust to controlling for both local temperature and rainfall variation as well as global ENSO variation (Extended Data Fig. 5). When we restrict analysis to between-sibling comparisons, estimates remain large and positive but are noisier probably due to the substantially reduced variance in our explanatory variable.

For all specifications, instrumental variables estimates are larger than analogous ordinary least squares (OLS) estimates that simply regress local health outcomes on local $PM_{2.5}$ exposures and condition on the same fixed effects; these differences are statistically significantly different in the full Sub-Saharan African sample ($P = 0.02$ for the dust instrument) but only marginally statistically different for the West African sample ($P = 0.06$ for the dust instrument). Importantly, given our instrumental variables strategy, our estimates represent 'local average treatment effects'[25], which is the average effect of $PM_{2.5}$ on child health for those individuals for whom changes in dust emission over the Bodélé cause changes in local $PM_{2.5}$ exposure. Our estimates thus do not represent treatment effect estimates for other types or sources of $PM_{2.5}$ exposure nor estimates for regions where variation in $PM_{2.5}$ is not driven by emission from the Bodélé.

Discussion

Our estimates of the effect of $PM_{2.5}$ on infant mortality are greater than the largest previously published empirical estimates for all

of Sub-Saharan Africa[13]. There are several potential explanations for this difference. First, if local economic activity worsens pollution but improves health outcomes, estimation strategies that do not explicitly account for this covariation will underestimate the impact of pollution on health. Our instrumental variables strategy overcomes this challenge by directly isolating variation in pollution exposure from variation in local economic activity. Second, classical measurement error in local measures of $PM_{2.5}$ exposure will bias OLS estimates of the effect of $PM_{2.5}$ on health toward zero, a problem that is corrected by instrumental variables estimation if the instrument is uncorrelated with the local measurement error[26]. In our setting, and particularly for our rainfall instrument, this condition is plausibly met, providing another reason why instrumental variables estimates are larger than least squares estimates. Consistent with these explanations, our instrumental variable estimates for Africa are comparable in magnitude to other quasi-experimental estimates from elsewhere in the world (Fig. 3b), nearly all of which come from developed or middle-income countries where exposures are often more precisely measured. Our results are also corroborated by other studies that use different measures of particulate exposure to examine the effect of dust exposure on health and economic outcomes in West Africa[14]. Taken together, these estimates clearly indicate that air pollution is a critical determining factor for child health around the world and that improvements in air quality can be expected to cause large improvements in child health.

In our African setting, our results highlight the particular importance of air pollution that is non-anthropogenic in origin and suggest two broad pathways for reducing the health burden of this exposure. A first approach would be to better understand how local interventions, ranging from personalized protective equipment to early warning systems, might reduce individuals' dust exposure in downwind inhabited areas. A second approach would be to better understand the existing and potential future controls on emissions at their Bodélé source. These could include both known climate controls as well as prospective direct efforts to mitigate emissions at source locations.

Regarding the climate channel, our results, and much past work[16,19,23,24,27], suggest that climate variation is a key control on dust export from the region. Because anthropogenic climate change is projected to have large potential influence on these patterns[28,29], altering the trajectory of future climate change could have large effects on child health across the continent through its impact on the emission and transport of Saharan dust. To our knowledge, the potential importance of this channel has not been recognized or explored.

To illustrate this channel's potential importance, we calculate projected changes in rainfall over the Bodélé by mid-century (2035–2065) relative to a 1995–2015 baseline, using 36 models from the Coupled Model Intercomparison Project Phase 5 (CMIP5) archive run under the representative concentration pathway 8.5 (RCP 8.5) emissions scenario. As has been previously characterized[18,28,30], rainfall projections over the regions are highly uncertain, with the ensemble median projected rainfall change close to zero but with individual models drying or wetting by more than 25% during Harmattan months (Fig. 4a). Incorporating uncertainty in both how Bodélé rainfall affects local $PM_{2.5}$ and in how local $PM_{2.5}$ affects mortality, these rainfall changes imply a large spread in potential changes in infant mortality due to changes in dust exposure (Fig. 4b,c), ranging from a –13% decline in mortality (5th percentile estimate) for models projecting precipitation increase to a 12% increase in mortality by mid-century (95th percentile) for models that dry. To our knowledge, these potential impacts are substantially larger than any known projected health impact of climate change on the continent. These findings suggest that better understanding the current and evolving future climatic constraints on Saharan dust export, including vegetation and precipitation feedbacks that may

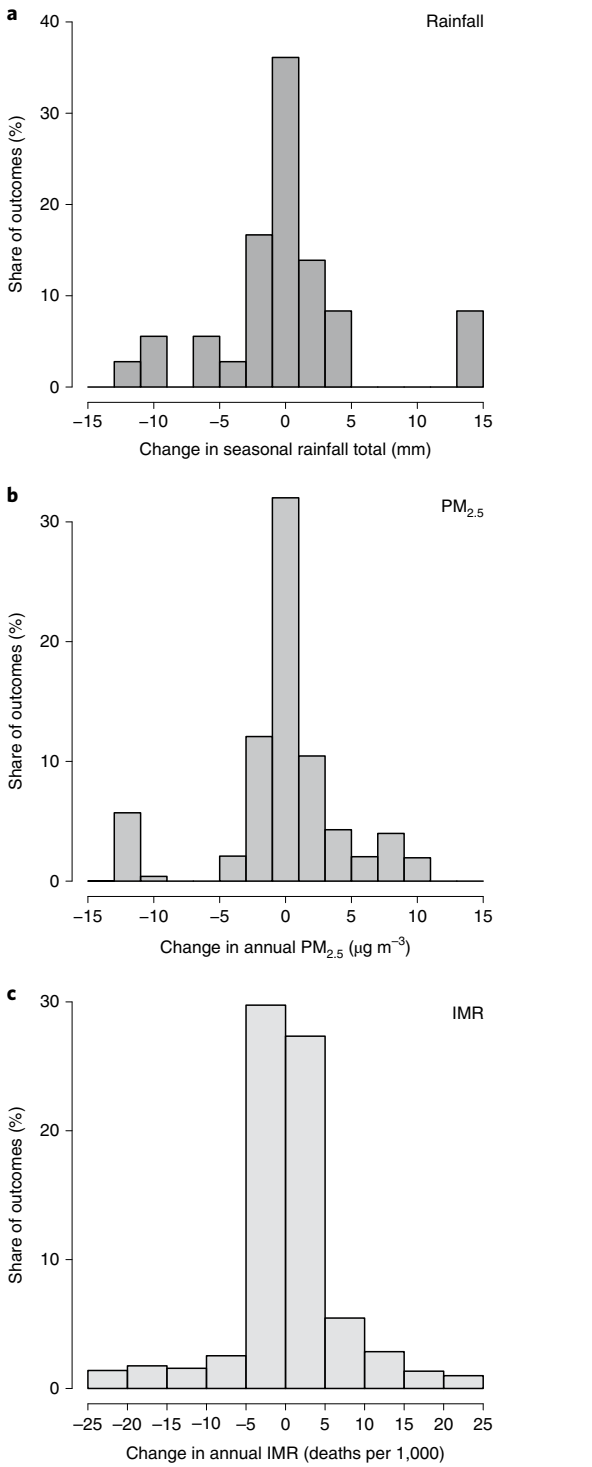

Fig. 4 | Disagreement among climate model projections of future rainfall changes in the Sahara generates a large spread in projected infant mortality changes in Africa. a, Projected changes in rainfall levels (2045–2055 relative to 2000–2015) over the Bodélé Depression during the Harmattan season (November–April) across 36 climate models. Baseline average rainfall during these months is 43 mm. **b**, Projected changes in $PM_{2.5}$ across West Africa in response to rainfall changes shown in **a**, incorporating uncertainty in both the distribution of rainfall projections and in the statistical relationship between rainfall in the Bodélé and local $PM_{2.5}$ across West Africa (see Methods). **c**, Changes in infant mortality rate (IMR) resulting from the changes in $PM_{2.5}$ modelled in **b**. Distribution of outcomes represents uncertainty in $PM_{2.5}$ changes as well as uncertainty in the relationship between $PM_{2.5}$ and infant mortality.

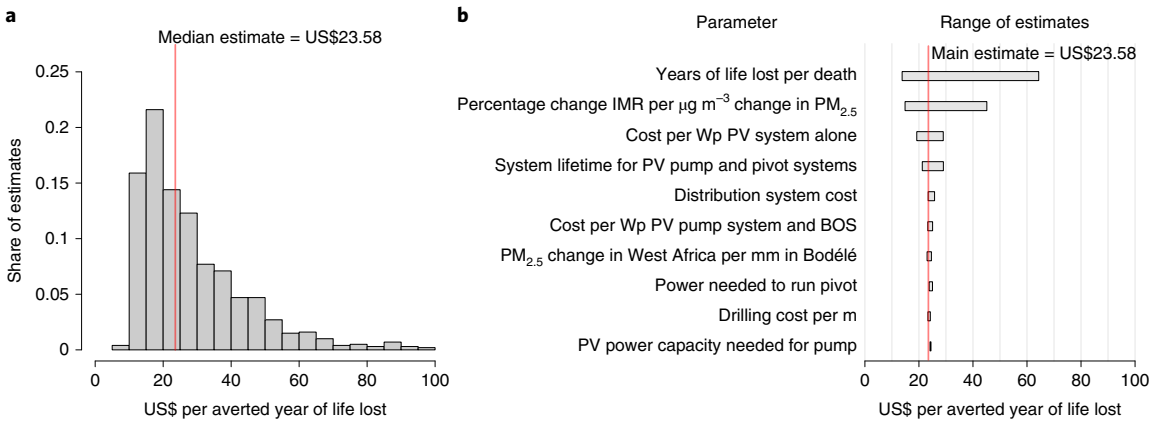

Fig. 5 | Cost per averted life-year lost under an intervention using pumped groundwater to reduce dust export from the Bodélé. a, Distribution of estimated cost per averted year of life lost, with a median value of US$24 (shown by red dotted line) and a 95% CI of US$11–75. Distribution was calculated by repeatedly sampling parameters with defined uncertainty (see Methods and Extended Data Table 1). The mean estimate is US$32 per averted year of life lost. **b**, Sensitivity of cost estimates to parameter values. For each parameter with a defined range of uncertainty, the parameter was fixed at its minimum (maximum) value and all other parameters were repeatedly sampled and median cost estimates were calculated for the minimum value and maximum value of the fixed parameter. Bars show the range of cost estimates when fixing the parameter at its minimum and maximum values, respectively. Cost estimates depend most heavily on the assumed years of life lost per death and on the estimated response of the infant mortality rate (IMR) to changes in $PM_{2.5}$. Wp, watts peak; PV, photovoltaic; BOS, balance of system.

be poorly represented in models[16,31–33] and the large influence of changing wind strengths and patterns on dust export[16], remains a key scientific and policy priority.

Because mitigating dust exposure, particularly for infants, would be extremely difficult (many houses have open windows or permeable roofs or walls, and infants and young children cannot or will not wear masks), direct efforts to mitigate dust emission from Bodélé also warrant future evaluation. In particular, existing estimates of even small amounts of renewable groundwater resources in the region[34], combined with proven technologies currently deployed in the Sahel that use renewable power to bring this water to the surface[35], suggest that local groundwater could potentially be used to dampen the surface and mitigate lofting of dust aerosols from Bodélé, reducing downwind exposures and health burdens. Analogous interventions have been used successfully to suppress dust emissions at small scale in California, using shallow flooding for near-complete mitigation of dust emission from important emission sites[36].

To explore this possibility, we estimate the costs and benefits of deploying solar-powered central pivot irrigation in the Bodélé, using our estimates of how a millimetre of additional water reduces downwind mortality, combined with conservative estimates of recharge and flow rates, equipment and operational costs, and assumptions of how averted infant deaths are converted to lost life-years (see Methods). We calculate a cost per averted life-year lost of US$24 (95% CI: US$11–75; Fig. 5), which even if low by a factor of five, is well below cost thresholds designating 'priority' interventions in low-income countries. For instance, the World Health Organization recommends that any intervention costing less than per capita GDP is 'very cost effective' (their highest designation)[37], and average per capita incomes in West Africa range from ~US$400 in Niger to ~US$2,000 in Ghana and Nigeria. Pumping groundwater to reduce dust export also appears cost competitive with many leading health interventions currently in use, including a range of vaccines, water and sanitation interventions and behavioural interventions[38].

While this calculation clearly ignores other plausibly important constraints to project deployment, such as logistical and political impediments to operating in remote and insecure environments in the Sahara, or operationalizing the deployment of irrigation during wind events, our intent is to suggest that such projects, if feasible, could yield enormous benefits at a modest cost. Better understanding the technical, economic and political constraints—as well as potential climate[32,39] and biogeochemical[40] impacts—of the deployment of such a system is a promising avenue for future work.

Methods

A description of the main methods used in the analysis are provided here and additional details are available in Supplementary Information.

Data. *Infant mortality data.* Data on infant health outcomes are taken from the DHS, nationally representative surveys that are conducted in many low-income and middle-income countries. DHS have a two-stage design, whereby a number of clusters are first selected from a list of enumeration areas created in a recent population census, and then households are randomly selected in each of the clusters, and women aged 15–49 yr are selected from those households for in-depth surveys. In most survey waves, enumerators use global positioning system devices to collect geospatial information to identify the central point of the populated area of each cluster[11]. We used data from all 65 surveys available at the time of writing that were carried out between 2001 and 2015 to reconstruct a village-level birth history. Our sample covers 30 countries and includes 990,696 individual birth outcomes (Extended Data Fig. 1). The outcome of interest for this study is infant mortality, which is represented by a dummy variable equal to one when a child was reported to die within the first 12 months following birth. Children who were alive but less than 12-months-old at the time of the survey were not included in our sample. The mean infant mortality rate in our sample is 71 deaths per 1,000 births.

$PM_{2.5}$ data. For our main analysis, we use data on $PM_{2.5}$ from the Atmospheric Composition Analysis Group at Dalhousie University. These data incorporate retrievals from MODIS AOD as well as other satellite instruments and models (MISR, SeaWIFS, GEOS-Chem) to estimate annual bias-corrected average surface $PM_{2.5}$ concentrations at high spatial resolution (down to $0.01^{\circ} \times 0.01^{\circ}$) with global coverage[10]. We use this data product along with an analogous product produced by the same group that uses models to subdivide estimates of $PM_{2.5}$ into natural (dust and sea salt) and non-natural sources. Non-natural source $PM_{2.5}$ is estimated by applying simulated compositional information following the process described in Van Donkelaar et al.[22]. We emphasize that the dust $PM_{2.5}$ data we use are a combination of information from satellites (to obtain total aerosols), from statistical models (to relate total aerosols to surface $PM_{2.5}$) and from transport models and emissions inventories (to separate dust from non-dust $PM_{2.5}$). There is undoubtedly considerable uncertainty in these data, particularly regarding dust concentrations. However, given existing limitations, we believe these data provide the best available estimates of $PM_{2.5}$ and dust concentrations across Africa. Moreover, we note that these data use the enhanced MODIS Deep Blue AOD for aerosol retrievals over the desert as well as the MAIAC algorithm. MODIS Deep Blue was specifically designed for bright desert surfaces[41] while the MAIAC algorithm is a high spatial resolution complement to the Deep Blue data that is also designed to perform especially well over bright desert surfaces because it uses

historical time-series information to help distinguish clouds and other transient phenomena and accounts for major land surface reflectance changes that take place in regions like the Sudano-Sahel.

$PM_{2.5}$ and its natural component are extracted for each year for all study locations as well as the Bodélé (Extended Data Fig. 1). We emphasize that satellite-derived $PM_{2.5}$ concentrations over the Bodélé are a proxy, rather than a direct measure, of dust emission from the area, and probably capture some dust transport into the area from nearby regions. As described below, what is key for our analysis is that these sources of Saharan dust are uncorrelated with local factors in our study region thousands of miles away.

To study the daily propagation of dust from the Bodélé across Africa (Extended Data Fig. 2), we use a recent global dataset of daily DAOD also derived from MODIS AOD[20]. We do not use these data for our main analysis because of the coarse spatial resolution and large numbers of missing values.

Rainfall data. High-resolution remote sensing based gridded rainfall data come from the Climate Hazards Group InfraRed Precipitation with station data (CHIRPS)[42]. CHIRPS incorporates satellite imagery with ground station observations to estimate monthly rainfall totals globally at 0.05°×0.05° spatial resolution. We sum monthly rainfall data across the post-birth period described above separately for where observed births occur and in the Bodélé Depression. Mean annual rainfall totals are 123 cm in our study locations and 4 cm in the Bodélé Depression.

Constructing $PM_{2.5}$ exposure. For each birth, we estimate the dust instrument by multiplying the share of total $PM_{2.5}$ from natural sources in the DHS cluster with $PM_{2.5}$ concentrations in the Bodélé in the 12 months following the birth. The share of total $PM_{2.5}$ from natural sources is estimated by first subtracting $PM_{2.5}$ with dust and sea salt removed from total $PM_{2.5}$ and then dividing by total $PM_{2.5}$. For the rainfall instrument we replace the Bodélé $PM_{2.5}$ concentration with the sum of monthly rainfall totals in the Bodélé over the same period. For OLS (also used in the first stage of the instrumental variable approach) we estimate total $PM_{2.5}$ concentrations by simply retrieving the total $PM_{2.5}$ concentration in the DHS cluster for the same time period. Given that $PM_{2.5}$ data are only available annually, we calculate $PM_{2.5}$ concentration in period t as the weighted averages of the annual data, where the weights represent the share of the year that falls into the time period. For example, a child born in the third month of year t would be assigned a post-birth concentration of (10/12)[concentration in year t] + (2/12)[concentration in year $t+1$].

Estimation. To isolate the causal effect of $PM_{2.5}$ exposure on infant health, we use an instrumental variables/two-stage least squares strategy. In contrast to an OLS estimator where infant health is regressed directly on local pollution, here we use plausibly exogenous variation in local $PM_{2.5}$ driven by distant dust emission to identify the impact of $PM_{2.5}$ exposure on health. Our specific strategy is analogous to shift-share instruments commonly used in economics[43], where we combine spatial variation in average exposure levels with time-series variation in a source of exposure. For the spatial variation, we calculate the share of $PM_{2.5}$ that comes from non-anthropogenic sources, averaged over our 2001–2015 study period. The mean share of $PM_{2.5}$ from natural sources in our sample is 42% and varies from 0% in parts of East Africa to 97% in parts of West Africa (Fig. 1b). For the time-series variation, we use either time variation in $PM_{2.5}$ concentrations in the Bodélé Depression or cumulative rainfall over the Bodélé. The mean 12-month average $PM_{2.5}$ concentration in the Bodélé Depression is 75 $\mu g\,m^{-3}$ in our sample but varies between 65 and 80 $\mu g\,m^{-3}$ (Fig. 1c). Mean cumulative rainfall over the same period is 4.3 cm in our sample and varies between 4.0 and 5.0 cm (Fig. 1d). Our instrument is then constructed by multiplying the spatially varying shares of $PM_{2.5}$ from natural sources in all locations i with either the time-varying dust concentrations or cumulative rainfall in the Bodélé Depression across time periods t.

Two-stage least squares/instrumental variables regression proceeds in two steps. In the 'first stage', the potentially endogenous regressor of interest (in our case, local measurements of $PM_{2.5}$ exposure over time) is regressed on the instrument and all other controls. Then, in the second stage, the outcome of interest (in our case, infant mortality) is regressed on the the predicted values from the first stage as well as the controls.

Our first-stage regression linking distant dust export to local $PM_{2.5}$ exposure is then:

$$PM_{ijcmt} = \lambda DV_{it} + \mu \mathbf{X}_{ijcmt} + \gamma_j + \delta_t + \nu_{cm} + \varepsilon_{ijcmt} \quad (1)$$

where PM_{ijcmt} denotes the post-birth total $PM_{2.5}$ exposure for individual i in cluster j, country c, born in month and year mt. $DV_{it} = (\phi_j \times D_t)$ is our instrument equal to the share of $PM_{2.5}$ from dust in cluster j (ϕ_j) times dust export from the Bodélé in year t (D_t). The estimated coefficient λ measures the effect of dust (or rainfall) in the Bodélé, weighted by share of $PM_{2.5}$ from dust, on overall local $PM_{2.5}$ concentrations. We also include a vector of individual, household and village-level controls $\mathbf{X}$, which include: local rainfall and temperature in time period t, night-time lights in time period t, a dummy for whether the household uses clean cooking fuel, a dummy for whether mother completed primary school, mother's age and age-squared at time of child's birth, child sex, child's birth order and a dummy for whether the child was a twin. Fixed effects (dummy variables) are included for each DHS cluster (γ_j), birth year (δ_t) and country–month (ν_{cm}) in our main specification. Our instruments are very strong, with first-stage F statistics > 100 (Fig. 2a) and are consistent across combinations of fixed effects, household controls and instruments (Extended Data Fig. 4; see Supplementary Information for further discussion on interpretation of first-stage results).

In the second stage, we regress infant mortality on predicted values of local $PM_{2.5}$ exposure from equation (1):

$$y_{ijcmt} = \beta \widehat{PM}_{ijcmt} + \mu \mathbf{X}_{ijcmt} + \gamma_j + \delta_t + \nu_{cm} + \varepsilon_{ijcmt} \quad (2)$$

where y_{ijcmt} is a binary measure of whether individual i survived to his/her first birthday. Equation (2) includes the same fixed effects and controls in $\mathbf{X}$ as equation (1). The fixed effects isolate variation in $PM_{2.5}$ exposure from other time-invariant, seasonally varying, or time-trending factors that could be correlated with mortality. In particular, inclusion of cluster fixed effects accounts for any time-invariant unobservables that could be correlated with both $PM_{2.5}$ exposure and mortality risk at the cluster level (for example, any location-specific differences in mortality rates due to average incomes or healthcare access), inclusion of country–month fixed effects accounts for any seasonal differences across locations within a country (for example, if mortality rates are higher in June than January in Nigeria) and time fixed effects account for any abrupt or trending factors common across the sample (for example, the overall decline in infant mortality over the last 15 yr). As an alternate specification, we can include mother fixed effects instead of cluster fixed effects in equations (1) and (2). In this specification, the effect of $PM_{2.5}$ exposure on mortality is derived by comparing two siblings born at different times to the same mother (Extended Data Fig. 5). This strategy further reduces the possibility of unobserved confounders, at the cost of eliminating much of the variation in exposure across the sample.

For estimates of $\hat{\beta}$ in equation (2) to represent causal estimates of the impact of $PM_{2.5}$ on infant health, it must be the case that, conditional on controls, our instrument is uncorrelated with other factors beyond local $PM_{2.5}$ exposure that also affect infant health. While this restriction is untestable, we directly include a vector of controls $\mu \mathbf{X}_{ijcmt}$ meant to address potential additional sources of confounding. In particular, one concern is that global or regional climate phenomena could affect both dust emission over the Bodélé as well as local meteorological conditions, and that these latter conditions could themselves shape health outcomes (for example, local drought lowering food availability). To account for this, we control directly for both temperature and rainfall locally, as well as for the global time series of Pacific sea surface temperature anomalies, the main index used to measure ENSO (Extended Data Fig. 5). A remaining failure of the exclusion restriction would have to involve large-scale climate phenomena that are not picked up either by these global indices or by local meteorological conditions and we are unaware of any such phenomena that fit this description.

Finally, we emphasize that $\hat{\beta}$ estimates the local average treatment effect[25] of $PM_{2.5}$ exposure, which in our setting is the average effect of $PM_{2.5}$ on child health for those individuals for whom changes in dust emission over the Bodélé cause changes in local $PM_{2.5}$ exposure. Our estimates thus cannot be assumed to represent treatment effect estimates for other types or sources of $PM_{2.5}$ exposure nor estimates for regions where variation in $PM_{2.5}$ is not driven by emission from the Bodélé.

Placebo tests. To ensure that the strong estimated first-stage relationship between variation in remote dust emission and variation in local $PM_{2.5}$ concentrations is not simply driven by either common time trends or common shocks across dusty locations or by average spatial differences between dusty and less-dusty locations, we conduct a placebo exercise where we randomly reorder either the time series of dust emissions over the Bodélé or the spatial shares of baseline levels of dust exposure and re-estimate the relationship between these placebo instruments and local-level $PM_{2.5}$ concentrations. In all cases, estimates on these placebo samples (n = 1,000 for each type of reshuffling) are close to zero (Fig. 2a,b), suggesting our estimated relationship between local $PM_{2.5}$ concentrations and remote dust emission is not spurious. The reason that we conduct this placebo exercise for the first-stage (equation (1)) and not for the full instrumental variable (IV) estimation (equations (1) and (2)) is that manually adding uncertainty to our instruments creates an artificially weak first stage and inflates the IV estimates. For a single instrument the estimated IV coefficient is equal to the reduced form coefficient (that is, the coefficient associated with regressing infant mortality on our instrument directly) divided by the first-stage coefficient. Randomly reordering the elements of our instrument and causing the first-stage coefficient to be close to zero mechanically causes the IV estimates to be large. We therefore compare the magnitude of first-stage coefficients, rather than IV coefficients, for the placebo samples.

Climate change simulations. To understand the impact of changing precipitation under future climate conditions, we examine rainfall projections over the Bodélé Depression using 36 climate models run under RCP 8.5. For each model we calculate average daily rainfall levels for the baseline period 1995–2015 and for the future period 2045–2055. Average daily rainfall totals were then summed across the Harmattan season and changes in seasonal rainfall were estimated as (future

rainfall) – (baseline rainfall). Half of the models (18 of 36) were found to project an increase in rainfall while the other half project a decrease. The distribution of predicted rainfall changes is shown in Fig. 4a.

Using our historical data, we estimate that a 1-mm increase in rainfall in the Bodélé during the Harmattan season reduces $PM_{2.5}$ in West Africa by 0.71 $\mu g\,m^{-3}$. This estimate comes from a grid-cell level regression where annual $PM_{2.5}$ in our West Africa study locations is regressed on season rainfall totals in the Bodélé Depression. The regression includes cell fixed effects to control for time-invariant differences over space and country-specific linear and quadratic time trends to control for country-specific trends in either rainfall or $PM_{2.5}$ over time. Cells are weighted by population. To characterize the uncertainty associated with the rainfall–$PM_{2.5}$ relationship we estimate the bootstrap distribution by sampling locations with replacement and re-estimating the coefficient 1,000 times. Combining these bootstraps with rainfall projections from the 36 climate models, we get 36,000 estimated changes in $PM_{2.5}$ shown in Fig. 4b. While the median change in $PM_{2.5}$ is zero, the inner 95% of projected changes range from 12 $\mu g\,m^{-3}$ reduction to 9 $\mu g\,m^{-3}$ increase in $PM_{2.5}$.

We then use our main model for West Africa (equation (2)) to estimate the change in infant mortality rate associated with changes in local $PM_{2.5}$ concentrations, again bootstrapping this estimate 1,000 times. Combined with the bootstrap sampling of the 36,000 changes in $PM_{2.5}$ concentrations, we get 36 million estimated changes in infant mortality (Fig. 4c). The median change in infant mortality is zero but the inner 95% range of the distribution of projected impacts spans a 19 deaths per 1,000 reduction (–23% relative to baseline) to a 16 deaths per 1,000 increase (+20%).

Mitigation of dust emission damages. We simulate the use limited renewable groundwater resources in and near the Bodélé depression to dampen the surface of the emission region during the Harmattan season and reduce infant deaths through reduced downwind air pollution. Analogous systems have been used successfully to suppress emissions in places like Owens Lake in the United States[36,44–47]. To estimate the cost-effectiveness of this type of system we draw on available estimates on local dust emission, sustainable recharge and flow rates of local aquifers, depth-to-groundwater, equipment and operational costs for solar PV and pumping equipment, and assumptions of how deaths are converted to lost life-years. Baseline estimate and uncertainty ranges for each parameter and the exact calculations are shown in Extended Data Table 1 and described further in Supplementary Information. We calculate that a reasonable solar-based dampening system would avert 37,000 infant deaths in West Africa annually. Our baseline estimate assumes that infants whose death before reaching age 1 yr has been averted live, on average, 30 healthy life-years (and therefore the averted death also averts 30 disability-adjusted life-years). Combined with cost estimates, this yields a cost-effectiveness estimate of US$23.58 per averted year of life lost.

To assess uncertainty in these estimates we assign upper and lower bounds to as many parameters as possible (Extended Data Table 1) and sample from these distributions to generate a range of estimates. Parameter estimates from the literature are sampled uniformly between their upper and lower bounds while parameters that come from regression estimates in this paper are sampled from a normal distribution with mean equal to the regression coefficient and standard deviation equal to the estimated coefficient standard error. We sample from each of the parameters with defined uncertainty 1,000 times and calculate the cost per averted year of life lost. The median estimate is US$24 per averted year of life lost and the 95% CI US$11–75 (Fig. 5a). We also assessed individual parameters' influence on the overall estimates (Fig. 5b). For each parameter with a defined range of uncertainty, the parameter was fixed at its minimum (maximum) value and then all other parameters were repeatedly sampled and median cost estimates were calculated. Estimates depend most heavily on the assumed years of life lost per death followed by the change in infant mortality as a response to changes in $PM_{2.5}$. Cost estimates are stable even with substantial increases in our assumed cost of infrastructure.

Even the highest end of our estimates would make efforts to reduce dust emissions high-value interventions by any benchmark for low-income countries and would be cost competitive with many leading health interventions[38]. While this calculation clearly ignores other potential constraints to project deployment, such as logistical and political impediments to operating in remote and insecure environments in the Sahara, our intent is to suggest that such projects, if feasible, would yield enormous benefits at a modest cost.

We also note other key uncertainties and feedbacks absent from our calculation, the inclusion of which could possibly improve the efficacy of a wetting intervention beyond what we estimate here. For instance, recent work suggests that large-scale deployment of solar power over the Sahara could increase local rainfall[39] and highlights a potential negative feedback between dust emission and rainfall[31,32]. We also note that our estimate of the effect of wetting is based on the measured effect of rainfall on dust but rainfall both wets the soil as well as scavenges dust in the air; a ground irrigation system would only do the former. Understanding these impacts and feedbacks is an important avenue for future research.

Data availability

Data are available at https://github.com/burke-lab/NatSus2020.

Code availability

Code to replicate all results is available at https://github.com/burke-lab/NatSus2020.

Received: 20 August 2019; Accepted: 26 May 2020;
Published online: 29 June 2020

References

1. Shindell, D., Faluvegi, G., Seltzer, K. & Shindell, C. Quantified, localized health benefits of accelerated carbon dioxide emissions reductions. *Nat. Clim. Change* **8**, 291–295 (2018).
2. Burnett, R. et al. Global estimates of mortality associated with long-term exposure to outdoor fine particulate matter. *Proc. Natl Acad. Sci. USA* **115**, 9592–9597 (2018).
3. Lelieveld, J., Haines, A. & Pozzer, A. Age-dependent health risk from ambient air pollution: a modelling and data analysis of childhood mortality in middle-income and low-income countries. *Lancet Planet. Health* **2**, e292–e300 (2018).
4. Cesur, R., Tekin, E. & Ulker, A. Air pollution and infant mortality: evidence from the expansion of natural gas infrastructure. *Econ. J.* **127**, 330–362 (2017).
5. Arceo, E., Hanna, R. & Oliva, P. Does the effect of pollution on infant mortality differ between developing and developed countries? Evidence from Mexico City. *Econ. J.* **126**, 257–280 (2016).
6. Chay, K. Y. & Greenstone, M. *Air Quality, Infant Mortality, and the Clean Air Act of 1970* Working Paper No. 10053 (National Bureau of Economic Research, 2003).
7. Knittel, C. R., Miller, D. L. & Sanders, N. J. Caution, drivers! children present: traffic, pollution, and infant health. *Rev. Econ. Stat.* **98**, 350–366 (2016).
8. Chay, K. Y. & Greenstone, M. The impact of air pollution on infant mortality: evidence from geographic variation in pollution shocks induced by a recession. *Q. J. Econ.* **118**, 1121–1167 (2003).
9. He, G., Fan, M. & Zhou, M. The effect of air pollution on mortality in China: evidence from the 2008 Beijing Olympic Games. *J. Environ. Econ. Manag.* **79**, 18–39 (2016).
10. Van Donkelaar, A. et al. Global estimates of fine particulate matter using a combined geophysical-statistical method with information from satellites, models, and monitors. *Environ. Sci. Technol.* **50**, 3762–3772 (2016).
11. Aliaga, A. & Ren, R. *Optimal Sample Sizes for Two-stage Cluster Sampling in Demographic and Health Surveys* Working Paper No. 30 (DHS, 2006).
12. Miller, G. & Urdinola, B. P. Cyclicality, mortality, and the value of time: the case of coffee price fluctuations and child survival in Colombia. *J. Polit. Econ.* **118**, 113–155 (2010).
13. Heft-Neal, S., Burney, J., Bendavid, E. & Burke, M. Robust relationship between air quality and infant mortality in Africa. *Nature* **559**, 254–258 (2018).
14. Adhvaryu, A. et al. Dust and death: evidence from the West African Harmattan. *Econ. J.* (in the press).
15. Foreman, T. *The Effect of Dust Storms on Child Mortality in West Africa* Working Paper No. 47 (CDEP-CGEG, 2018).
16. Evan, A. T., Flamant, C., Gaetani, M. & Guichard, F. The past, present and future of African dust. *Nature* **531**, 493–495 (2016).
17. Koren, I. et al. The Bodélé Depression: a single spot in the Sahara that provides most of the mineral dust to the Amazon forest. *Environ. Res. Lett.* **1**, 014005 (2006).
18. Washington, R. et al. Dust as a tipping element: the Bodélé Depression, Chad. *Proc. Natl Acad. Sci. USA* **106**, 20564–20571 (2009).
19. Wagner, R., Schepanski, K., Heinold, B. & Tegen, I. Interannual variability in the Saharan dust source activation—toward understanding the differences between 2007 and 2008. *J. Geophys. Res. Atmos.* **121**, 4538–4562 (2016).
20. Voss, K. K. & Evan, A. T. A new satellite-based global climatology of dust aerosol optical depth. *J. Appl. Metereol. Climatol.* **59**, 83–102 (2020).
21. Washington, R. & Todd, M. C. Atmospheric controls on mineral dust emission from the Bodélé Depression, Chad: the role of the low level jet. *Geophys. Res. Lett.* **32**, L17701 (2005).
22. Van Donkelaar, A., Martin, R. V., Brauer, M. & Boys, B. L. Use of satellite observations for long-term exposure assessment of global concentrations of fine particulate matter. *Environ. Health Perspect.* **123**, 135–143 (2015).
23. Brooks, N. & Legrand, M. in *Linking Climate Change to Land Surface Change* (eds McLaren, S. J. & Kniveton, D. R.) 1–25 (Springer, 2000).
24. Wang, W., Evan, A. T., Lavaysse, C. & Flamant, C. The role the Saharan heat low plays in dust emission and transport during summertime in North Africa. *Aeolian Res.* **28**, 1–12 (2017).
25. Angrist, J. & Imbens, G. Identification and estimation of local average treatment effects. *Econometrica* **62**, 467–475 (1994).
26. Angrist, J. D. & Krueger, A. B. Instrumental variables and the search for identification: from supply and demand to natural experiments. *J. Econ. Perspect.* **15**, 69–85 (2001).

27. Wang, C., Dong, S., Evan, A. T., Foltz, G. R. & Lee, S.-K. Multidecadal covariability of North Atlantic sea surface temperature, African dust, Sahel rainfall, and Atlantic hurricanes. *J. Clim.* **25**, 5404–5415 (2012).
28. Biasutti, M. Forced Sahel rainfall trends in the CMIP5 archive. *J. Geophys. Res. Atmos.* **118**, 1613–1623 (2013).
29. Skinner, C. B. & Diffenbaugh, N. S. Projected changes in African easterly wave intensity and track in response to greenhouse forcing. *Proc. Natl Acad. Sci. USA* **111**, 6882–6887 (2014).
30. Rodríguez-Fonseca, B. et al. Variability and predictability of West African droughts: A review on the role of sea surface temperature anomalies. *J. Clim.* **28**, 4034–4060 (2015).
31. Yoshioka, M. et al. Impact of desert dust radiative forcing on Sahel precipitation: relative importance of dust compared to sea surface temperature variations, vegetation changes, and greenhouse gas warming. *J. Clim.* **20**, 1445–1467 (2007).
32. Yu, K., D'Odorico, P., Bhattachan, A., Okin, G. S. & Evan, A. T. Dust–rainfall feedback in West African Sahel. *Geophys. Res. Lett.* **42**, 7563–7571 (2015).
33. Wang, W., Evan, A. T., Flamant, C. & Lavaysse, C. On the decadal scale correlation between African dust and Sahel rainfall: the role of Saharan heat low-forced winds. *Sci. Adv.* **1**, e1500646 (2015).
34. MacDonald, A. M., Bonsor, H. C., Dochartaigh, B. É. Ó. & Taylor, R. G. Quantitative maps of groundwater resources in Africa. *Environ. Res. Lett.* **7**, 024009 (2012).
35. Burney, J., Woltering, L., Burke, M., Naylor, R. & Pasternak, D. Solar-powered drip irrigation enhances food security in the Sudano-Sahel. *Proc. Natl Acad. Sci. USA* **107**, 1848–1853 (2010).
36. *2008 Owens Valley PM_{10} Planning Area Demonstration of Attainment State Implementation Plan* (Great Basin Unified Air Pollution Control District, 2008); https://go.nature.com/37qhRIP
37. *Macroeconomics and Health: Investing in Health for Economic Development* (Commission on Macroeconomics and Health, 2001).
38. Jamison, D. T. et al. *Disease Control Priorities* Vol. 9 (The World Bank, 2017).
39. Li, Y. et al. Climate model shows large-scale wind and solar farms in the Sahara increase rain and vegetation. *Science* **361**, 1019–1022 (2018).
40. Bristow, C. S., Hudson-Edwards, K. A. & Chappell, A. Fertilizing the Amazon and equatorial Atlantic with West African dust. *Geophys. Res. Lett.* **37**, L14807 (2010).
41. Hsu, N. et al. Enhanced Deep Blue aerosol retrieval algorithm: the second generation. *J. Geophys. Res. Atmos.* **118**, 9296–9315 (2013).
42. Funk, C. et al. The climate hazards infrared precipitation with stations—a new environmental record for monitoring extremes. *Sci. Data* **2**, 150066 (2015).
43. Bartik, T. J. *Who Benefits from State and Local Economic Development Policies?* (W.E. Upjohn Institute for Employment Research, 1991).
44. *Owens Valley PM_{10} Planning Area (OVPA) State Implementation Plan (SIP) Prior to the 2016 SIP* (Great Basin Unified Air Pollution Control District, 2014); https://gbuapcd.org/District/AirQualityPlans/SIP_Archive/
45. *Owens Valley PM_{10} State Implementation Plan* (Great Basin Unified Air Pollution Control District, 2016); https://gbuapcd.org/District/AirQualityPlans/OwensValley/
46. Gillette, D., Ono, D. & Richmond, K. A combined modeling and measurement technique for estimating windblown dust emissions at Owens (dry) Lake, California. *J. Geophys. Res. Earth Surface* **109**, F01003 (2004).
47. Groeneveld, D. P., Watson, R. P., Barz, D. D., Silverman, J. B. & Baugh, W. M. Assessment of two methods to monitor wetness to control dust emissions, Owens Dry Lake, California. *Int. J. Remote Sensing* **31**, 3019–3035 (2010).

Acknowledgements

We thank the National Science Foundation (CNH award no. 1715557) and the Robert Wood Johnson Foundation for funding. We also thank M. Greenstone for motivating comments on an earlier presentation.

Author contributions

M.B. and S.H.-N. conceived of the paper. S.H.-N., J.B., K.K.V. and M.B. analysed the data. All authors contributed to interpreting the results and writing the paper.

Competing interests

The authors declare no competing interests.

Additional information

Extended data is available for this paper at https://doi.org/10.1038/s41893-020-0562-1.

Supplementary information is available for this paper at https://doi.org/10.1038/s41893-020-0562-1.

Correspondence and requests for materials should be addressed to M.B.

Reprints and permissions information is available at www.nature.com/reprints.

Publisher's note Springer Nature remains neutral with regard to jurisdictional claims in published maps and institutional affiliations.

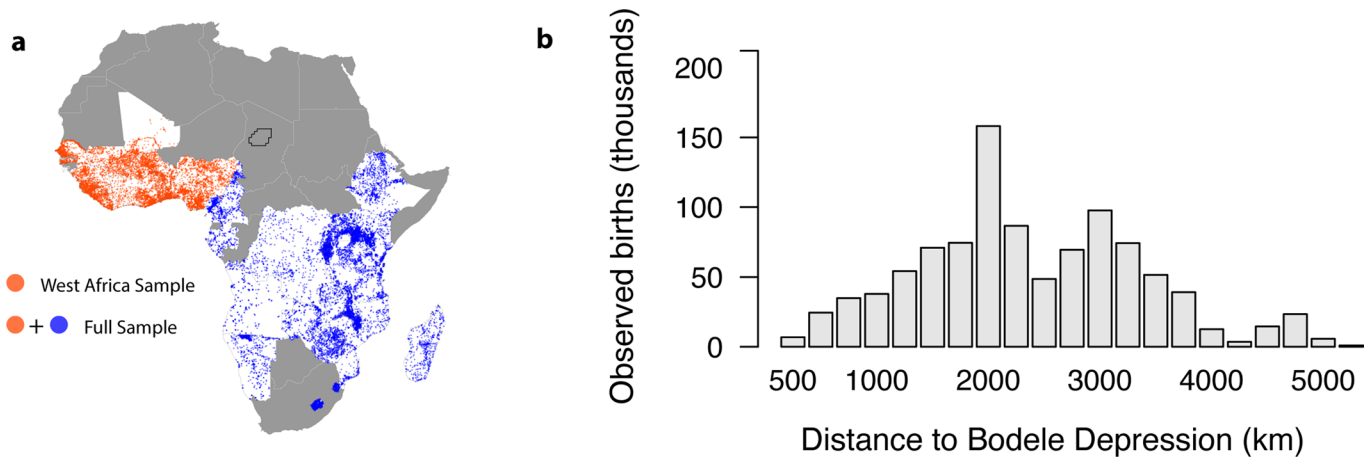

Extended Data Fig. 1 | Location of observed births and their distance to the Bodélé Depression. (a) Each point represents one of the 28,461 DHS clusters included in our sample. The number of observed births in a single cluster ranges from 1 to 210. Orange points indicate the West Africa sample. The full sample includes all points. The Bodélé Depression is outlined in black. (b) Observed births are 500-5000km away from the Bodélé Depression.

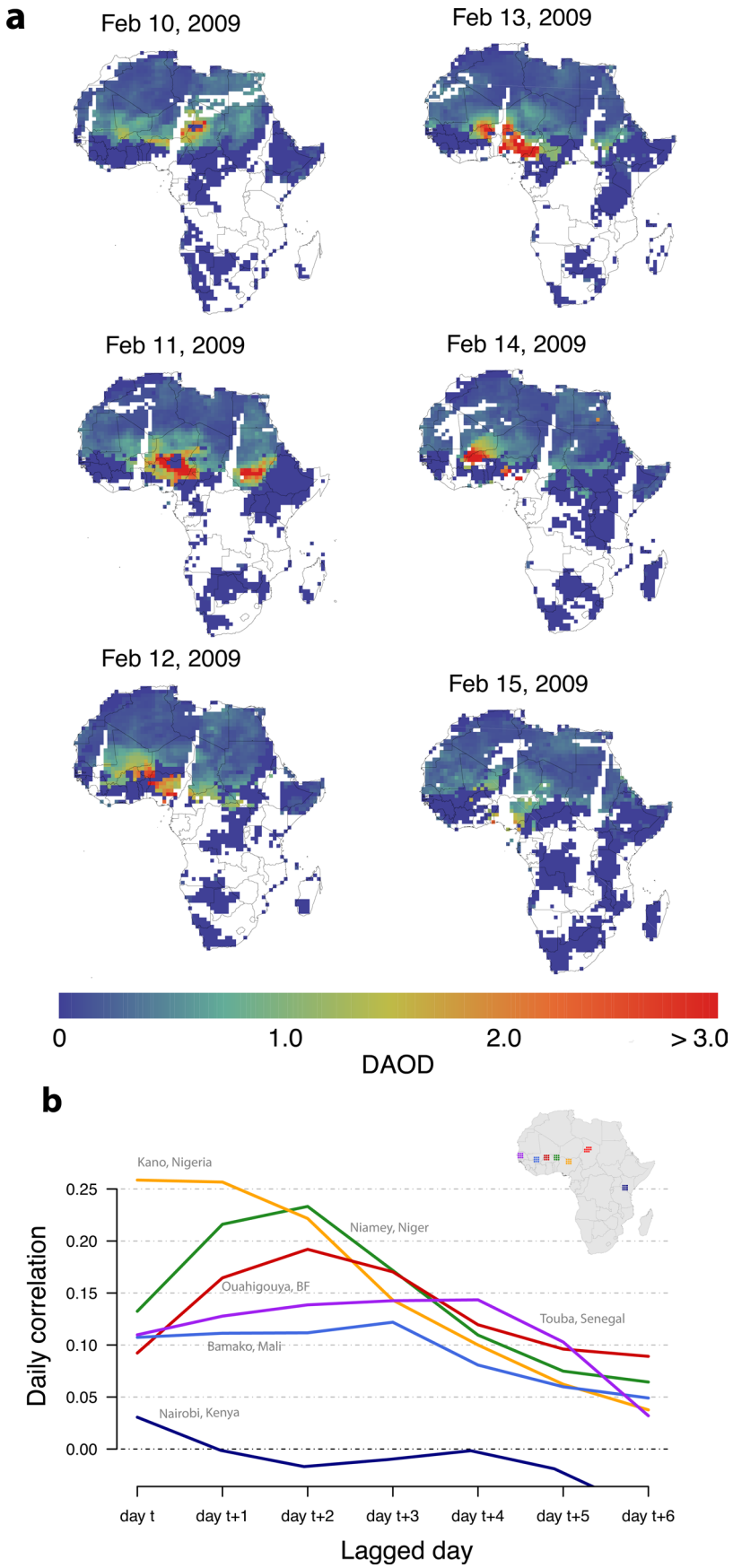

Extended Data Fig. 2 | See next page for caption.

Extended Data Fig. 2 | Dust is rapidly transported from the Bodélé Depression across West Africa and beyond and correlation of local dust concentration with Bodélé dust dissipates with distance. (a) Daily dust propagation, measured as Dust Aerosol Optical Depth (DAOD), over eight days during a large dust activation event illustrates the magnitude of dust concentrations as well as the timescale and spatial extent of transmission. Dust AOD ranges from 0 to greater than 3.0 in this example. For comparison, AOD values during the 2018 northern California wildfires were <1.0. (b) Detrended time series correlation of DAOD in the Bodélé Depression and DAOD at selected population centres dissipate over space and time. Map shows the location of selected population centres across West Africa as well as Nairobi, Kenya. Right panel shows the time-series correlation of detrended DAOD values between the mapped locations and the Bodélé Depression. In general, as distance to the Bodélé increases, peak correlations in the detrended DAOD time series occur later and are lower in magnitude. Variation in DAOD in Nairobi, a populated location distant and not downwind from the Bodélé, is uncorrelated with dust from the Bodélé.

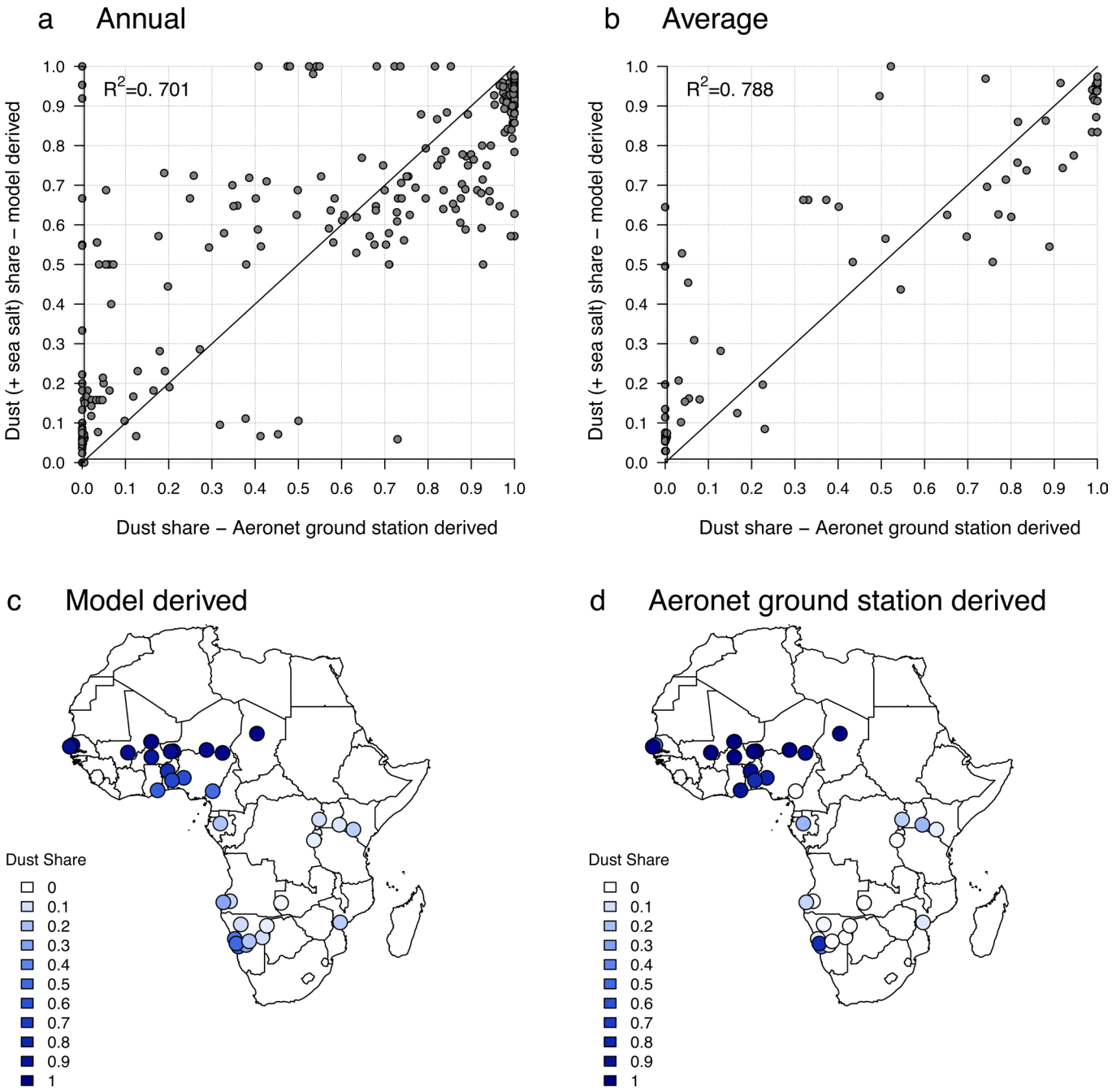

Extended Data Fig. 3 | Estimated shares of particulate matter from natural sources in the exposure data correlate well and exhibit similar spatial patterns with estimates of total aerosols from dust derived from Aeronet ground stations. For all Aeronet ground stations in our study countries with at least 3 years of data we estimated the share of total aerosols from dust (see Supplement) and compared them to the modelled share of total particulate matter from natural sources (dust and sea salt) for the same locations in the exposure data used in our analysis.[10] (a) Comparison of site by year shares. Despite the imperfect comparison between share of aerosols from dust to share of particulate matter from dust and sea salt, there is strong correlation between the data sets. The R^2 associated with regressing site by year share of particulate matter from natural sources on site by year share of aerosols from dust is 0.71. The largest discrepancies occur in coastal areas where the share of particulate matter from natural sources is dominated by sea salt. In those cases the share of particulate matter from natural sources can be close to 1 while the share of aerosols from dust can be close to 0. (b) Analogous to panel (a) but for long-run site averages instead of site-year observations. (c) Site average share of particulate matter from natural sources at locations of Aeronet sites in our study countries. (d) Site average share of aerosols from dust. For both data sets, shares are highest in West Africa where they are close to 1 for many locations.

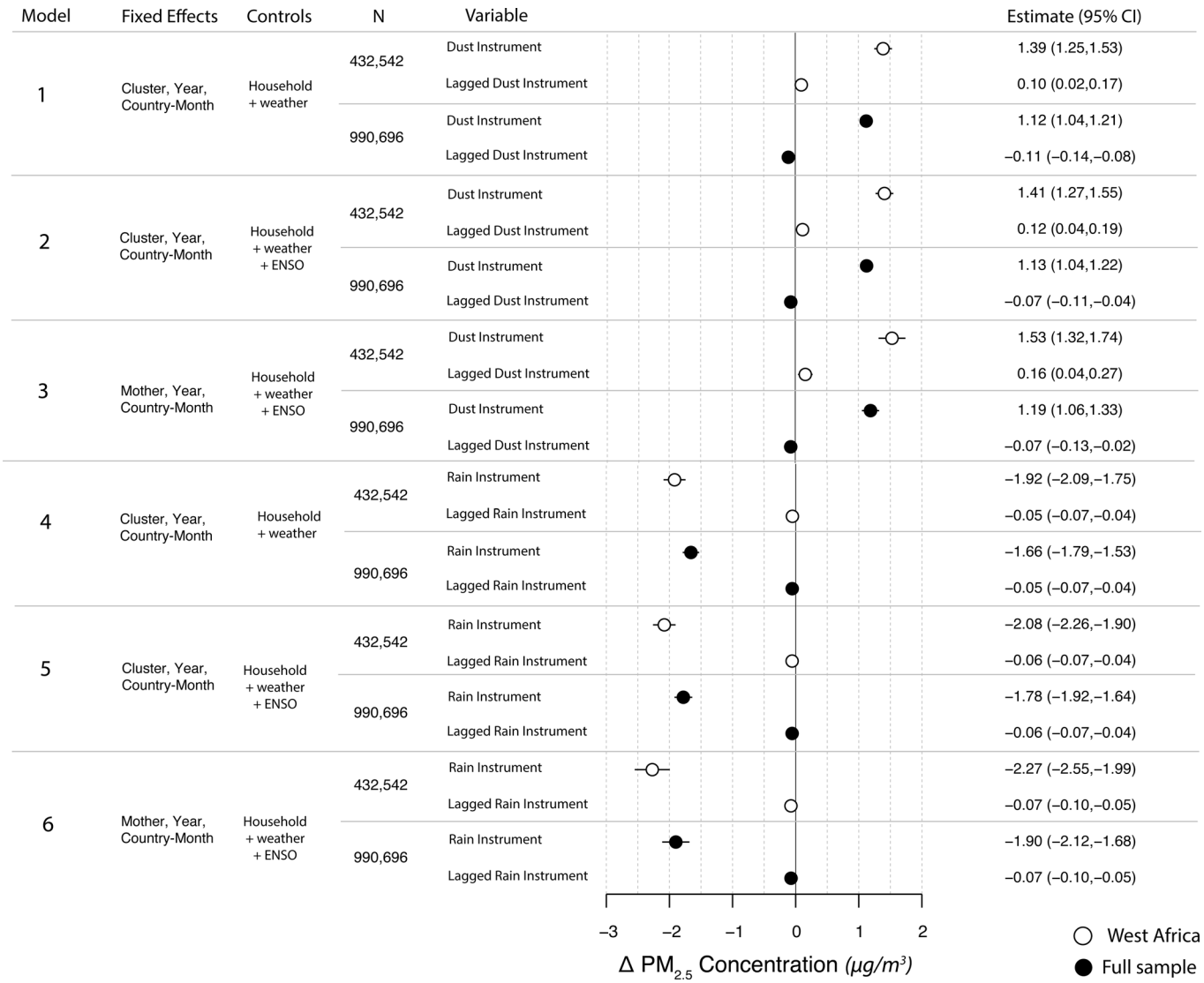

Extended Data Fig. 4 | Variation in dust concentration and rainfall over the Bodélé Depression are strong predictors of variation in $PM_{2.5}$ concentrations in other parts of Africa. Figure shows estimation results for six different specifications of the first stage (Eq. (1)) relationship between the conditions in the Bodélé instrument and local $PM_{2.5}$. Models 1 and 4 include DHS cluster, birth year, and country by month fixed effects with household and local weather controls and the dust (Model 1) or rainfall (Model 4) instrument. Models 2 and 5 add additional controls for ENSO conditions and Models 3 and 6 replace DHS cluster fixed effects with a mother fixed effect to restrict comparisons to siblings. The different specifications consistently find dust in the Bodélé Depression is positively associated and rainfall negatively associated with $PM_{2.5}$ concentrations in both our West African sample (white dots) and full African sample (black dots; see Extended Data Fig. 1 for study locations). Contemporaneous effects are large, statistically significant (F-stats of 17-366), and similar to the main specification without lags (Fig. 2) while lagged effects are small and not statistically significant. A complete description of the fixed effects (dummy variables) and controls is included in the Methods section.

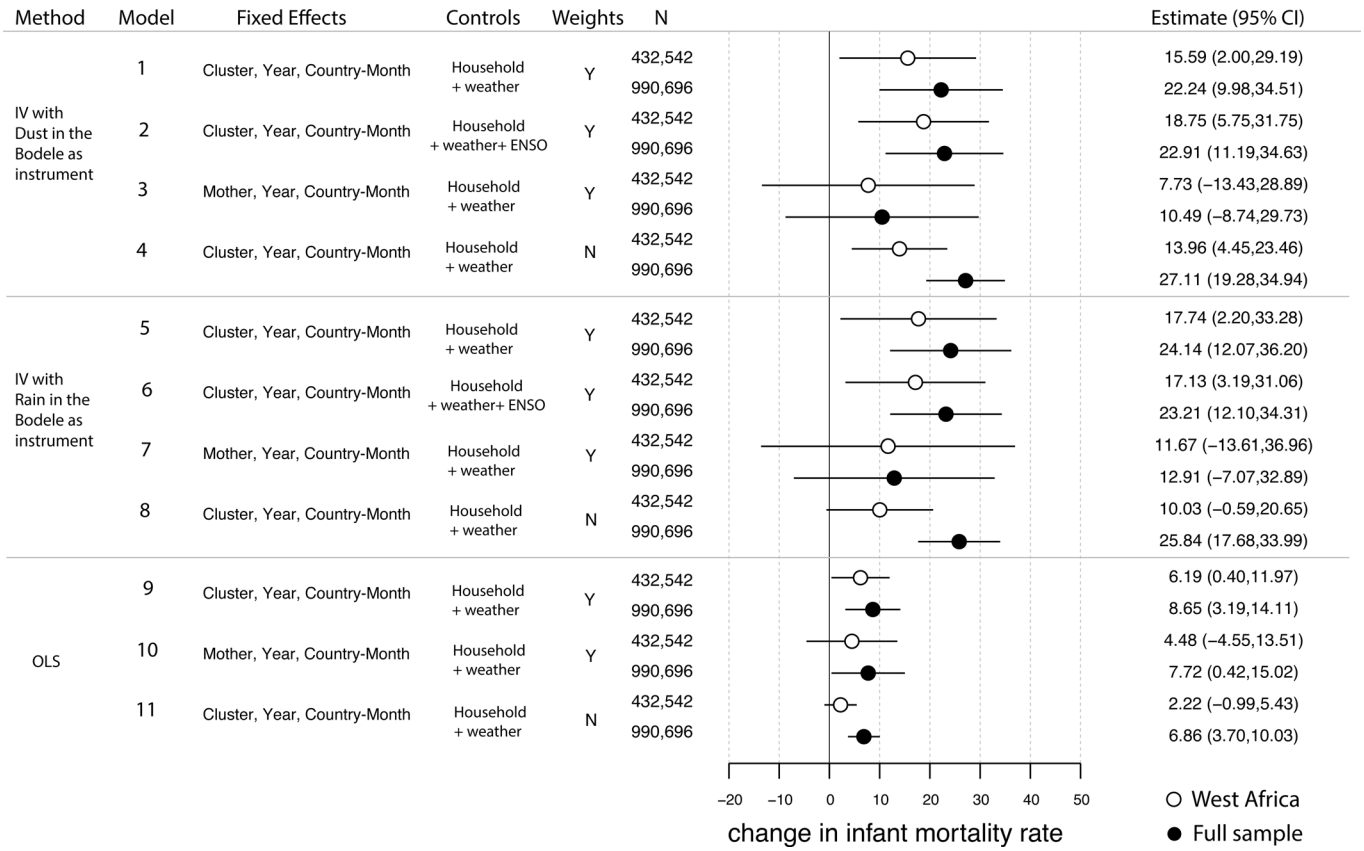

Extended Data Fig. 5 | Instrumental variable estimates of the effect of $PM_{2.5}$ on infant mortality are largely consistent across specifications. Effects on infant mortality are similar when we isolate variation in local $PM_{2.5}$ related to dust (Models 1-4) or rainfall (Models 5-8) over the Bodélé Depression. Models 1,5, and 9 include DHS cluster, child birth year, and country by month fixed effects with household and local weather controls (see Methods for details). Models 2 and 6 add controls for ENSO conditions. Models 3,7, and 10 replace DHS cluster fixed effects with mother fixed effects to limit the comparison to siblings. Models 4,8, and 11 drop the regression weights that account for survey sampling scheme and country population. Instrumental Variable (IV) estimates (Model 1-8) that isolate variation in local $PM_{2.5}$ exposure related to changes in Bodélé conditions are larger than the Ordinary Least Square (OLS) estimates that rely on all sources of variation in local $PM_{2.5}$ exposure (Models 9-11).

Table ED1: Overview of parameters used in cost calculations

	Cateogry	Parameter	Estimate	Lower Bound	Upper Bound	Units	Source
(1)	Desert	Bodele Area as defined in this paper	8.2E+10	NA	NA	m^2	This paper
(2)	Desert	Active Bodele Area Washington et al 2009	1E+10	NA	NA	m^2	Washington et al, PNAS 2009[18]
(3)	Groundwater	Average Depth to Groundwater	176	NA	NA	m	MacDonald et al, ERL 2012[34]
(4)	Groundwater	Average Flow Rate	12	NA	NA	L/s	MacDonald et al, ERL 2012[34]
(5)	Groundwater	Total Storage	36400	NA	NA	mm	MacDonald et al, ERL 2012[34]
(6)	Groundwater	Sustainable Recharge Rate	<5	NA	NA	mm/yr	MacDonald et al, ERL 2012[34]
(7)	Watering	Unit Area	6.4E+5	NA	NA	m^2	Based on standard centre pivot infrastructure
(8)	Watering	Water volume for 1mm over area	640	NA	NA	m^3	Based on standard centre pivot infrastructure
(9)	Watering	Pumping speed @ depth	10	NA	NA	m^3/day	Based on available Grundfos and Lorentz pump curves and (3)
(10)	Watering	Days per mm water	64	NA	NA	days	(8)/(9)
(11)	Borewell Drilling	Cost per m	100	80	120	$/m	Xenarios & Pavelic, Water SA 2013[60]
(12)	Solar PV Pumping System	Cost per Wp PV pump system & BOS	2.5	2	3.2	$/Wp	World Bank Solar Pumping Technical Report[61]
(13)	Solar PV Pumping System	PV power capacity needed for pump	3	2.5	3.5	kWp	Based on available Grundfos and Lorentz pump curves and (3)
(14)	Solar Center Piv. Irr. Sys.	Cost per Wp PV system alone	1	0.8	1.2	$/W	NREL Benchmarks;[62]
(15)	Solar Center Piv. Irr. Sys.	Distribution System Cost	3E+4	2E+4	4E+4	$	Based on standard centre pivot infrastructure
(16)	Solar Center Piv. Irr. Sys.	Power needed to run pivot	25	20	30	kWp	Based on standard centre pivot infrastructure
(17)	Solar Center Piv. Irr. Sys.	Number of pivots sharing power source	6	NA	NA	#	Design factor using (10) (14) (15)
(18)	Solar Center Piv. Irr. Sys.	System Lifetime for PV Pump & Pivot Sys.	25	20	30	years	Based on PV and pump literature
(19)	Solar Center Piv. Irr. Sys.	Borewell lifetime	50	NA	NA	years	Based on standard centre pivot infrastructure
(20)	Mortality	% Change IMR per μg/m3 change in PM2.5	2.43	1.24	3.62	percent	This Paper
(21)	Mortality	Baseline Mortality Rate for West Africa	81	NA	NA	per 100k	This Paper
(22)	Mortality	Births per Year	1.3E+7	NA	NA	births	This Paper
(23)	Mortality	$PM_{2.5}$ change in W. Africa per mm in Bodele	0.97	0.94	1.00	$\mu g/m^3$ per mm	This Paper
(24)	Mortality	years of life lost per averted death	30	10	46.8	years/death	WHO reportcommission2001macroeconomics & GHO Life tables
(25)	Outputs	Total Annualized Unit Cost	2018.68	NA	NA	$	[(3) x (11)]/(19) + [(12) x (13)]/(18)
(26)	Outputs	Fraction of area covered	1	NA	NA	%	(1)/(2)
(27)	Outputs	Number of units Needed	15625	NA	NA	units	[(26) x (2)]/(7)
(28)	Outputs	Total annualized cost	3.2E+7	NA	NA	$	(27) x (25)
(29)	Outputs	Total water over dry season	2	NA	NA	mm	min[150/(10),(6)]
(30)	Outputs	Average $PM_{2.5}$ reduction across W Africa	1.42	NA	NA	$\mu g/m^3$	(23) x (29)
(31)	Outputs	Averted deaths per year	32895.72	NA	NA	deaths	[(30) x (20) x (21) x (22)]/1000
(32)	Outputs	dollars per averted death	958.84	NA	NA	$/death	(28)/(31)
(33)	Outputs	dollars per averted YLL	31.96	NA	NA	$/year	(32)/(24)

Extended Data Table 1 | Overview of parameters used in cost calculations.